Indian Journal of Geo Marine Sciences
Vol. 52 (11), November 2023, pp. 531-544
DOI: 10.56042/ijms.v52i11.4908

Beach stage identification for Aksa beach (Malad, Mumbai) by analyzing wave dynamics, grain size distribution and morphodynamic characteristics

D B Gadkari* & S Das

Department of Geography, University of Mumbai, Mumbai, Maharashtra – 400 098, India

*[E-mail: gadkarideepali72@gmail.com]

Received 14 August 2023; revised 02 November 2023

Aksa beach, located in the eastern suburb of Mumbai near Malad is highly dynamic and experiences frequent spatial and temporal morphological changes, leading to sediment distribution issues and a high risk of drowning hazards. It is essential to identify the beach stage for effective beach management and reducing drowning risks. This study aims to assess the spatial and temporal morphological, sedimentological, and hydrodynamic characteristics of the beach to simplify determining its stage with morphodynamic features. Standard methods were used to collect and generate data related to variables such as slope, wave data, and sediment textural characteristics, which were analyzed using statistical techniques. To define the beach stage model, the study utilized two morphodynamic indices, fall velocity parameters (Ω) and Relative Tide Range parameters (RTR). Aksa Beach was classified as an intermediate reflective state with a Low Tide Bar (LTB) and rip current, which helps in risk assessment and beach management decisions. The beach stage model is a useful tool for understanding the morphodynamic systems of a beach, and it should be used for easy identification and management of drowning incidents and the beach environment.

[**Keywords**: Beach stage classification, Morphodynamic indices, Sediment dynamics, Wave dynamics]

Introduction

Beaches are an important component in protecting coasts from erosion by dissipating wave energy[1]. Due to their sensitivity to changes in wave energy, beaches can quickly adapt their shape with minor adjustments to the position of sand or shingle grains[2]. Several geomorphologists, such as Wright *et al.*[3], Wright & Short[4], and Masselink & Short[5], have identified various morphological stages of beaches associated with different wave and tide regimes. Wright & Short[4] developed a model that integrated hydrodynamic and morphological factors, which identified four intermediate domains separating dissipative and reflective domains. Masselink & Short[5] formulated a beach classification model considering waves, tides, and sediments. Woodroffe[6] described the dissipative to reflective domains in terms of wave energy. Dissipative beaches show high energy regime leading to excessive erosion from the upper and the lower parts of the beach. Due to excessive erosion, the steepness of the seaward side of a beach gets reduced and becomes gentle. This leads to increased deposition in the nearshore zone in the form of shore-normal bars or submersed hips/dunes of sediments. At the Aksa beach such shore-normal bars are observed at the southern part of Aksa beach. Troughs are created between the beach and these bars at approximately 3 – 4 m depth. Water at Aksa beach is deeper than the adjacent regions, where the surrounding areas have a depth of 1 – 2 m and the trough has a depth of 3 – 4 m. The beach swimmers do not have an idea about this increased depth of water and gets trapped and drowned.

Factors such as wave conditions, tides, currents, the nearshore zone extent, bars and troughs, beach morphology, and sediment characteristics (grain size) are considered when classifying beaches. In this study, Masselink & Short[5] model is applied to identify the stage of the Aksa beach based on its morphodynamics and hydrodynamics. The morphology and nearshore circulation of the Aksa beach change rapidly over short spatial-temporal scales, ranging from within one lunar cycle (1 – 15 days) to seasonal changes (pre-monsoon, monsoon, and post-monsoon). The locations of features such as sandbars in the nearshore zone, depressions on the beach, and sediments in the berm zone continuously change along the beach extent.

This research aims to establish a relationship between the morphodynamics, hydrodynamics and nearshore beach drowning hazards of Aksa beach and

identify the type of beach. The study will involve conducting topographic surveys of the beach before and after the monsoon season, measuring wave parameters, and studying the sediment dynamics by analyzing the sediment movement on and along the beach and the grain size distribution pattern.

Materials and Methods

Study area

The study area is located near Malad, one of the suburbs of Mumbai, India, with coordinates between latitude 19°10'38.19" N to 19°12'28.19" N and longitude 72°47'41.88" E to 72°48'21.88" E (Fig. 1).

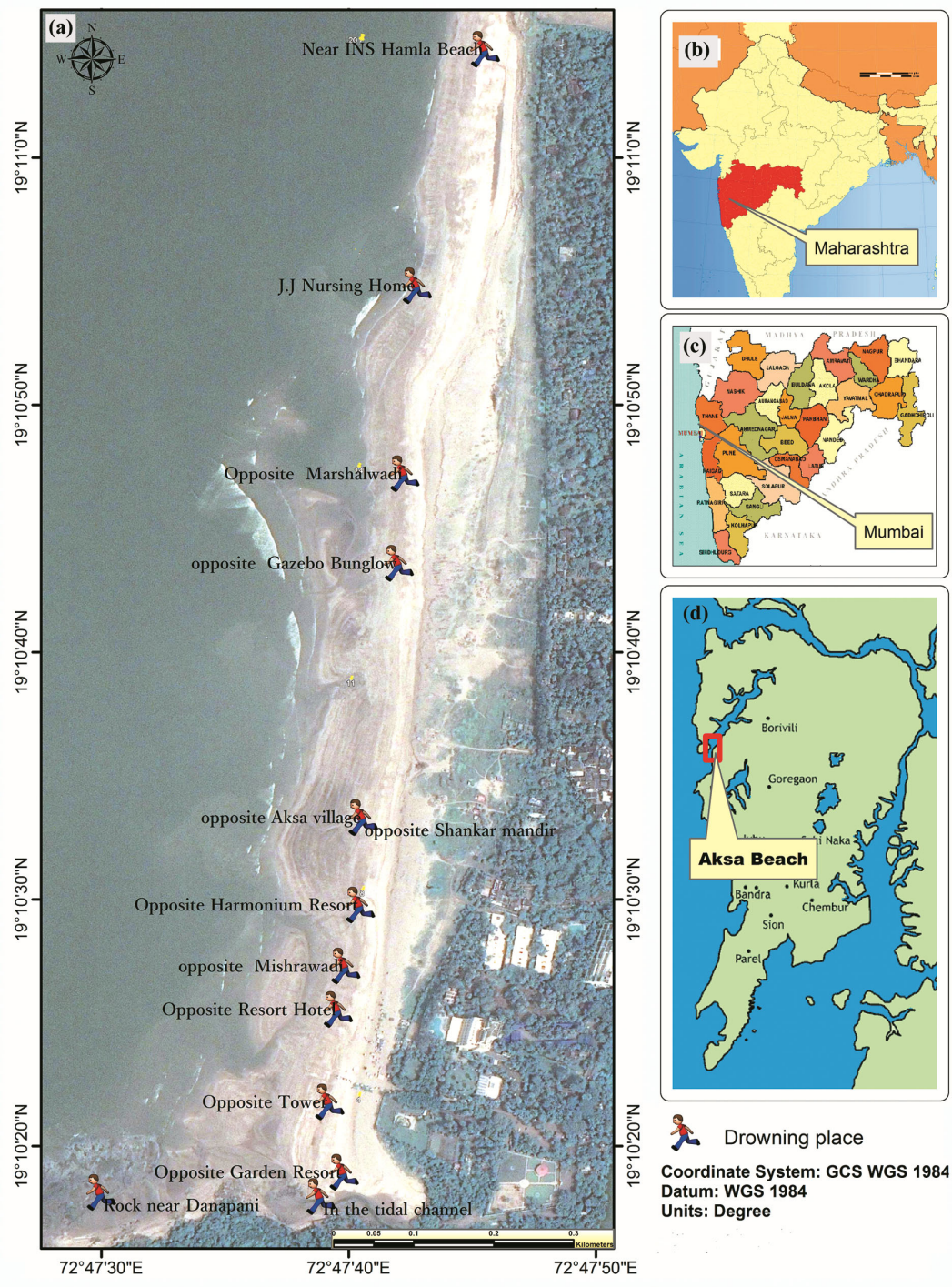

Fig. 1 — a) Location of drowning places at Aksa beach (Gadkari & Das, 2022)[6]; b) Maharashtra State from India map; c) Mumbai city in Maharashtra State; and d) Aksa beach in Mumbai

However, the area is also known for frequent drowning incidents. The study area has thirteen spots where drowning incidents have occurred, as shown in Figure 1(a).

Figure 2 shows the morphological map of the study area, highlighting the physical features of the beach. The beach is relatively straight compared to the adjacent beaches, with a sandy and smooth

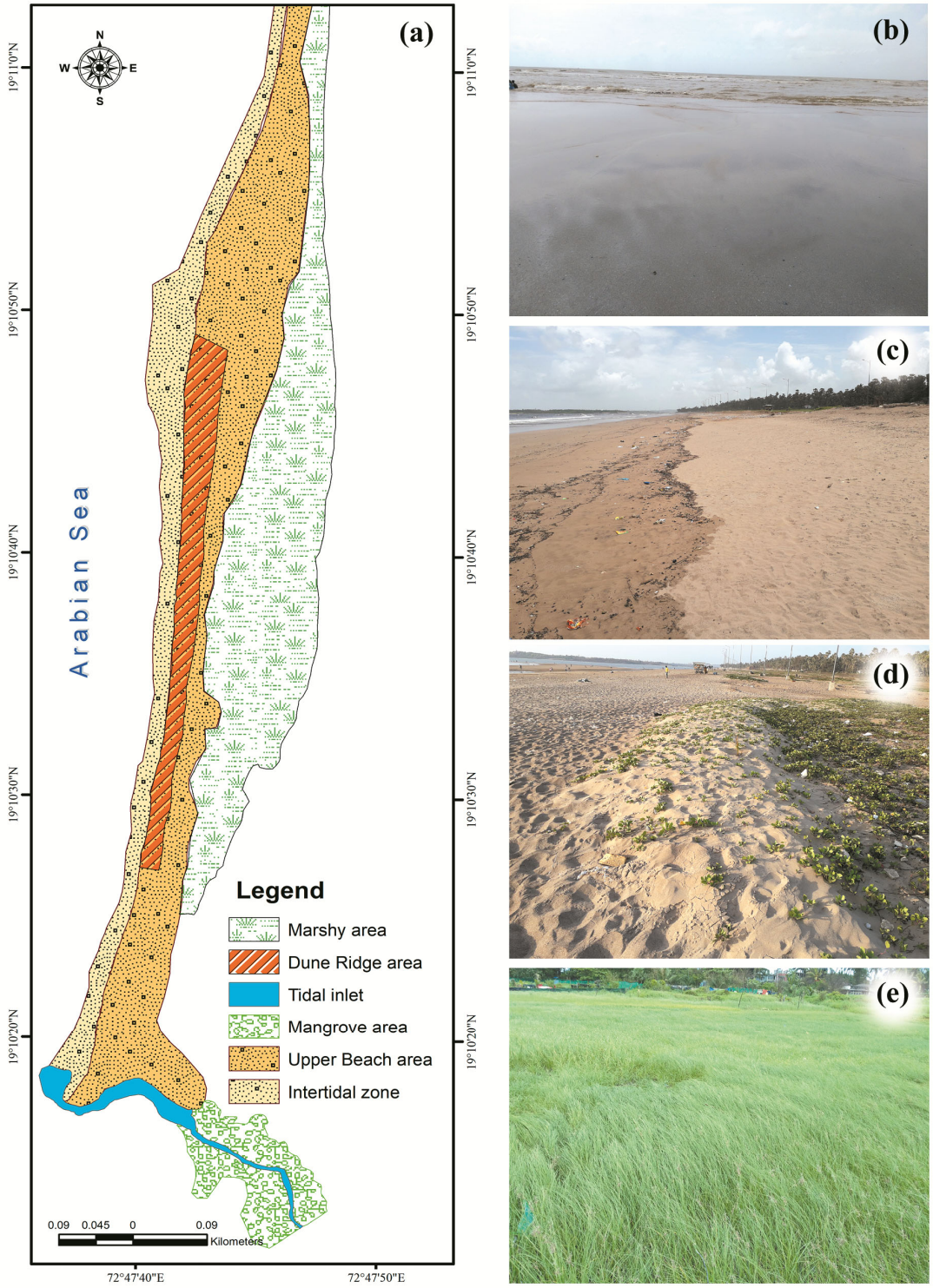

Fig. 2 — a) Morphological map of Aksa beach; b) Picture of the intertidal zone; c) Picture of the upper beach area; d) Dune ridge area; and e) Picture of marshy land area (Gadkari & Das, 2022)[6]

backshore bounded by a berm, embryonic dunes, and marshy land. The berm is a ridge of sand that marks the limit of the high tide zone. It is formed by the deposition of sand by waves and tides. The embryonic dunes are located behind the berm and are the first stage in the formation of dunes. They are small, undulating sand mounds held together by vegetation. The marshy land is located behind the dunes and is characterized by low-lying, waterlogged areas. These areas are dominated by salt-tolerant vegetation, such as mangroves.

Sand bars are present parallel to the beach and are exposed during low tide, with deep channels formed in the zones between these bars and the beach. These channels can be very dangerous for swimmers during high tide. The southern limit of the beach is marked by a tidal channel and a rocky shore platform, while Manori Creek marks the northern limit. Micro-geomorphic features such as berms, runnels, and ripple marks are also present despite macro-geomorphic landforms.

A tropical monsoon climate, with distinct wet and dry seasons, characterizes the climate of Aksa beach. The monsoon season typically lasts from June to September, when the region experiences heavy rainfall and strong winds. The prevailing winds in the study area are from the southwest during the monsoon season, while the rest of the year, the winds are predominantly from the northeast.

The atmospheric climate of the study area can significantly impact the wave climate, as the intensity and duration of monsoon rain and winds can change wave height (H), Wave period (T), and longshore direction (VI). Sea waves have a significant role in controlling the processes of beach morphology and sediment movement in the littoral areas[7]. At Aksa beach, the wave-fetch window is oriented between north 231.56° and north 222.42° (Fig. 3a), so the energy transfer from the wind to the sea is between the southwest and west direction with wind speed of up to 5 – 6 m/s. The wind data were obtained from the NASA Langley Research Center (LaRC) POWER Project, funded through the NASA Earth Science/Applied Science Program and collected data every month from 2006 – 2022 on 2023/10/26. Offshore wave data was obtained from the Versova buoy within the INCOIS Ocean Observation Network (OON) GUI, located offshore of Wave Rider Buoy (WRB)Versova (72°44'22" E, 19°07'92" N). The data collected by the Versova buoy effectively represents the offshore wave conditions in the study area. The data from 2016 to 2022 includes significant wave height and mean wave direction (Fig. 3b). The data show that the prevailing winds blow from southwest, where the average geographic fetch is equal to 8 km. The mean wave approaching the coast from southwest direction has a significant offshore height of 0.1 – 2 m (Fig. 3b). The highest wave with a significant offshore height greater than 3 m propagates from SW, where the geographic fetch reaches 7 – 8 km. It should be noted that the sea-wave measurements are offshore and can differ significantly nearshore due to shoaling effects, as explained by James[8]. The winds also blow from the southwest, with a speed of up to 5 – 6 m/s, generating waves nearshore because winds are onshore oriented. The data indicates that the study area experiences a relatively moderate-energy coastal environment, where during significant storms, high tide conditions, and the monsoon season, the washover phenomenon can impact the entire beach width.

The study area experiences waves primarily from the southwest, with an average wave height (H) of around 0.2 meters and an average wave period (T) of around 9 seconds. However, the wave height (H) and period can vary considerably depending on the season, with higher and more energetic waves during the monsoon season[9].

Beach topography

To study the general characteristics of the beach at Aksa in detail, the field visit has been carried out regularly from 2018 to 2022, either pre-monsoon or post-monsoon seasons. However, the Aksa beach was surveyed for its topography only at 2 times (May 2019 and October 2019). The physical sediment sampling was done in May 2019. The primary data of wave parameters through measurement was also collected 2 times (May 2018 and May 2019). The secondary data of offshore wave parameters was collected from 2006 – 2022. The period over which the records of drowning incidents are available are from 2006 to 2022. The topographic, elevation profile, and slope data were collected using a Total Station instrument and spatial locational data using a GPS device. The data were collected for the pre-monsoon season in May (2019) and the post-monsoon season in October (2019) along five transects (Fig. 4) from the northern to the southern side of Aksa beach. Profiles were measured from the dune to the lower beach at the points where there is break in slope observed along the beach.

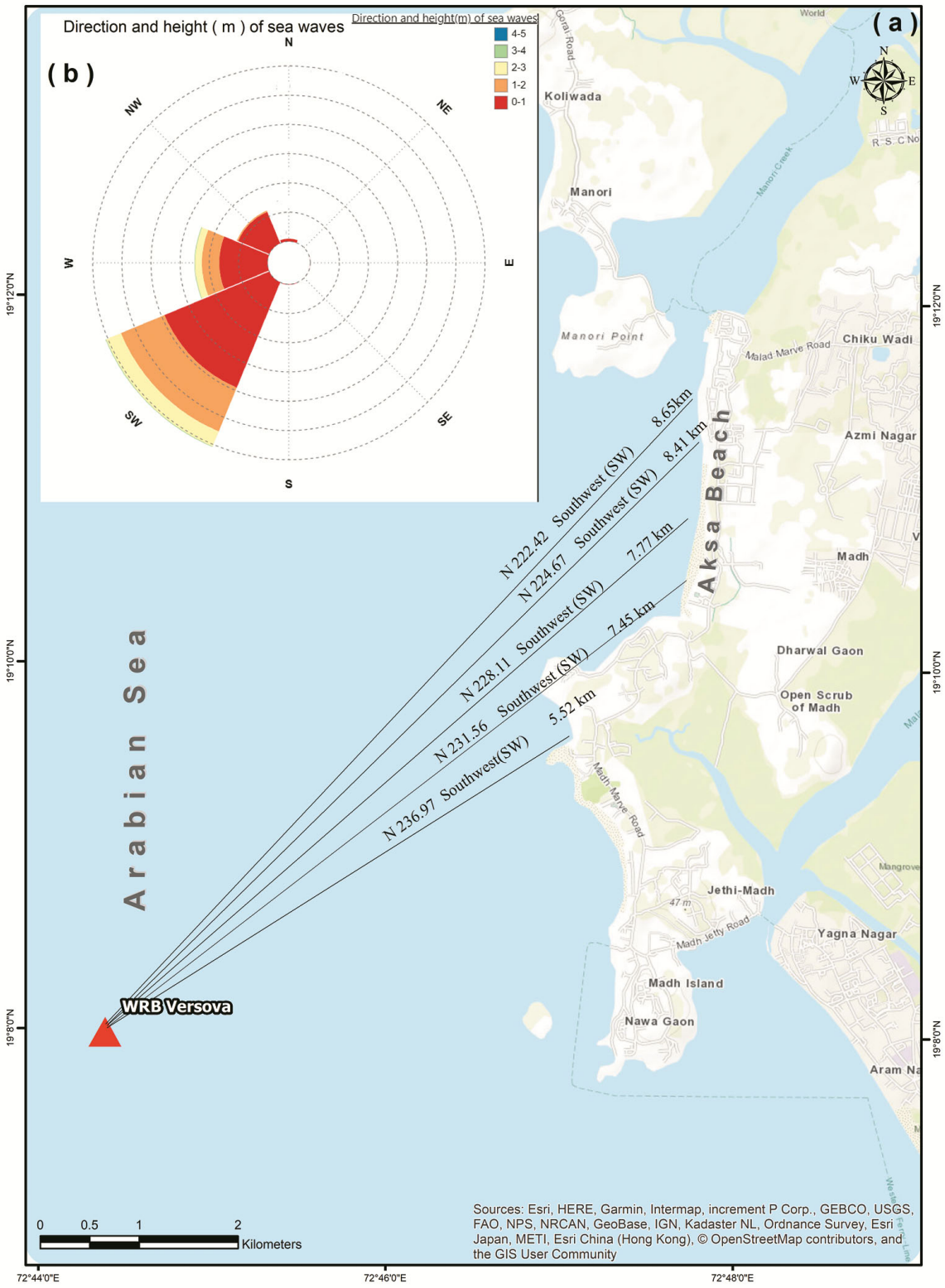

Fig. 3 — a) Wave fetch window at the Aksa beach, red triangle shows the location of the Versova buoy; and b) Wave height and mean wave direction obtained by the Versova buoy during the period 2016 – 2022

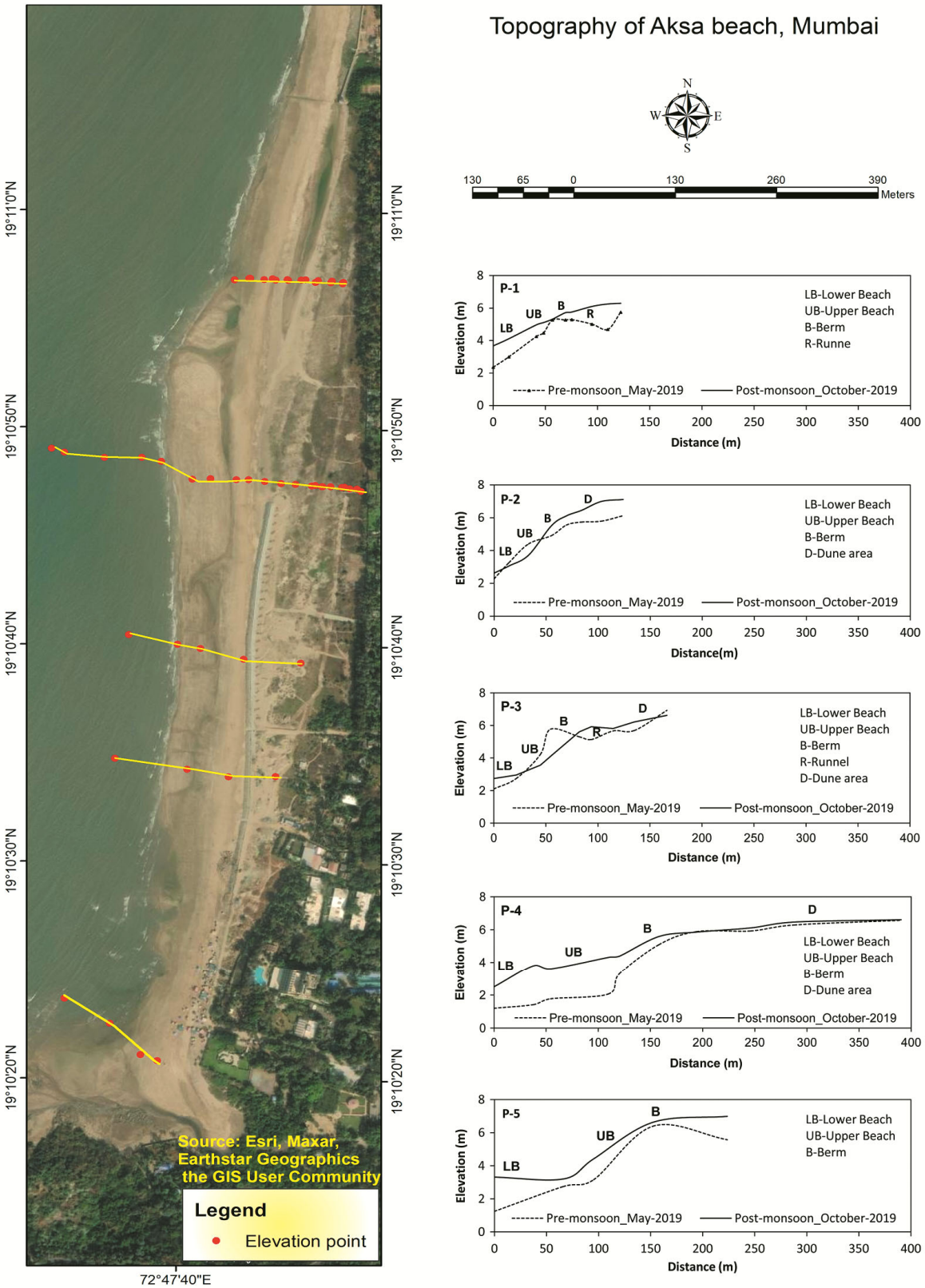

Fig. 4 — Profile of the Aksa beach, Mumbai

Comparing surveys taken along the same profile line on different seasons allows for identifying the magnitude of seasonal changes or short-term variations in the beach profile and the identification of longer-term erosional or accretional trends[10]. Spatial variations in beach profiles can also be assessed by comparing data collected on the same date from the adjacent profile lines along the shoreline[10].

Natural forces such as waves, tides, and currents are responsible for changes in beach profile[11-12]. The beach slope was measured using the uneven ground surface interval method over unequal distances corresponding to breaks or changes in slope[13]. After analyzing the data related to the slope of the beach, the morphological structure of the beach can be understood.

Textural analysis of sediments

In order to analyze the beach conditions and sediment transport processes, sediment texture is an essential factor to consider[14-15]. Sediment samples were collected along and across the beach from the backshore area to the lowest water level towards the seaward side, with a particular focus on points where there was a break in slope along the transects.

Fifty one sediment samples were collected along the beach profiles in May 2019. Sediment samples were collected from 51 different locations along cross profiles of the beach at a depth ranging from 20 to 40 cm from the surface to avoid surface impurities by hand sampling method. The standard method for dry-sieving outlined by Tucker[16] was used for textural analysis. The samples were dried and mechanically sieved. The sediment particle size data thus obtained was used as input data for specialised software "GRADISAT" [17]. This software facilitated an in-depth statistical analysis of the sorting index and mean grain size of the sediment samples. A nest of standard sieves at 0.5 ø intervals ranging from 4 mm to < 0.0625 mm was used. Using the Microsoft Excel-based program Gradistat-9.1, as explained by Blott & Pye[17], particle size measurements and statistical grain size distribution analyses were performed based on Folk & Ward[18] method. GRADISTAT 9.1, an open-source sediment grain size analysis software, was used to perform the statistical and graphical analysis. Central tendencies such as sorting index and mean grain size were obtained using the software[19].

Wave data

Wave parameter data was collected during the pre-monsoon (May) of the year 2018 and 2019 at the same location under similar tidal conditions for consistency in wave measurements. The data were analyzed for wave parameters such as wave height (H), peak period (T), wave frequency (F), and wavelength (L), which are compiled separately per year. For each parameter, the mean value was calculated for 2018 and 2019 and then the average between the two years was determined by taking the mean of the mean values for each parameter. Breaker height (Hb) was measured directly using a graduated staff to measure the distance from the water level to the wave crest. The wave period (T) was obtained by measuring the time (in seconds) for ten wave crests to pass a stationary object, such as a staff. Wavelengths (L) were measured directly using a measuring tape to determine the distance between two successive wave crests in meters. Longshore drift currents were measured by tracking the distance travelled by a float (e.g., an orange) over sixty seconds[20]. The direction of the longshore current was recorded using a fluorescent dye (Rhodamine B-$C_{28}H_{31}ClN_2O_3$)[21]. Wave velocity (C), wave steepness (H/L), and wave energy (E) values were calculated for the period of May 2018 and 2019 using equations 1 – 4 for 5 locations (Fig. 5) on the Aksa beach.

$$\textit{Wave velocity (C)} = L / T \text{ (ref. 22)} \quad \text{... (1)}$$

Where 'L' is wavelength and 'T' is Wave period

$$\textit{Wave steepness (H/L)} = H / L \text{ (ref. 22)} \quad \text{... (2)}$$

Where 'H' is wave height and 'L' is wavelength

$$\textit{Wave energy (E)} = 1/8\, pg\, H^2 \text{ (ref. 23)} \quad \text{... (3)}$$

Where 'p' is water density, 'g' is gravity, and 'H' is wave height

$$\textit{Breaker wave type} = Hb / Ws\, T \text{ (ref. 24)} \quad \text{... (4)}$$

Where, 'Hb' is the wave breaking height, 'Ws' is the potential fall velocity, and T is the wave period (T).

After collecting wave data, the mean values of each parameter across all five locations (Fig. 5) were calculated and summarised in Table 1. The average wave height (H) was 0.2 meters, the average wave period (T) was 9.02 seconds, and the average wave velocity (C) was 1.96 meters per second. The average wave steepness (H/L) was 0.03, and the average wave energy (E) was 56.91 Joules per square meter. The average wave frequency (f) was 7, and the average longshore drift velocity (VI) was 0.196 meters per second, as shown in Table 1. These data provide insight into the wave climate in the study area and how it varies across different locations. The data on wave climate is essential for understanding the wave and current conditions in the study area, which can significantly impact the beach morphology and sediment transport.

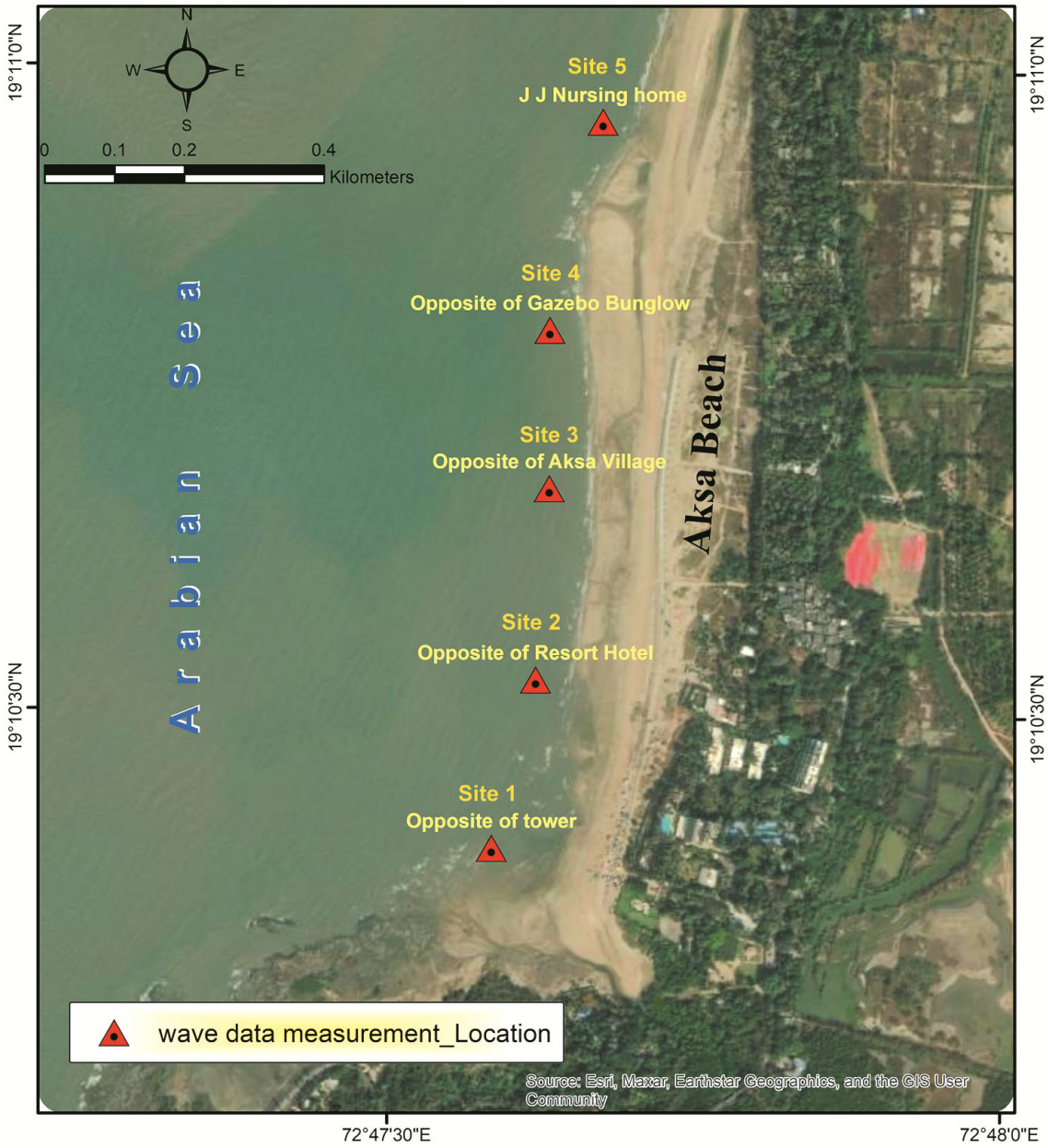

Fig. 5 — Locations of wave data measurement along the Aksa beach (Site 1 - Opposite of tower, Site 2 - Opposite of resort hotel, Site 3 - Opposite Aksa village, Site 4 - Opposite Gazebo bungalow, and Site 5 - J J nursing home)

Table 1 — Summary of mean wave and current data

	Wave height (H) in metres (m)	Wave period (T) in second (s)	Wave velocity (C) in (m/s) as seen in equation (1)	Wave steepness (H/L) as seen in equation (2)	Wave energy (Jule/m²) as seen in equation (3)	Wave frequency (f)	Longshore drift velocity (VI) (m/sec)
Site 1	0.16	8.7	1.77	0.033	31.07	8	0.23
Site 2	0.26	10.8	2.24	0.043	90.53	7	0.2
Site 3	0.16	9.25	1.9	0.025	33.96	8	0.2
Site 4	0.16	8.6	2.01	0.025	34.85	6	0.22
Site 5	0.24	7.75	1.9	0.026	94.12	8	0.13
Average	0.2	9.02	1.96	0.03	56.91	7	0.196

Beach stage model

To explain the high drowning risk at Aksa beach, the research used a beach safety evaluation model based on the beach morphodynamic state model proposed by Masselink & Short[5]. Figure 6 represents the beach morphodynamic state model. The model is based on the average values of dimensionless fall velocity parameters (Ω), as shown in equation 5 and Relative Tide Range parameters (RTR), as shown in equation 6.

$$\textit{Fall velocity parameters } (\Omega) = H_b/TW_s \quad \ldots (5)$$

Where, *Hb* = Wave breaking height; *T* = Wave period (T); *Ws* = Sediment fall velocity; *Ws* = *(RgD2)/[C1v+(0.75.C2.Rg.D3)0.5]*; *R* = Submerged specific gravity (1.65 for quartz); *D* = Sediment size; *v* (kinematic viscosity of the fluid) = μ/ρ, where μ is the dynamic (absolute) viscosity of the fluid is the density of the fluid, (the value of *v is* -1.0×10^{-6} $kg.m^{-1}.s^{-1}$ for water at 20 °C); *C1* = 18 constant; and *C2* = 1 constant.

$$\textit{Relative tide range parameters } (RTR) = TR/Hb \quad \ldots (6)$$

Where, *TR* = Mean spring tide range; and *Hb* = Wave breaking height.

The dimensionless fall velocity parameter (Ω) is calculated based on the wave parameters and the hydraulic properties of the sediment. The relative RTR is the ratio of the tidal range to the mean water depth.

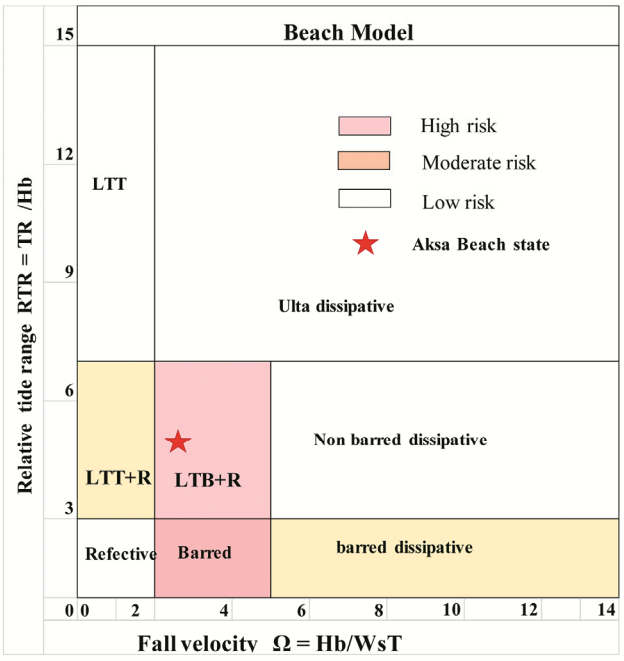

Fig. 6 — Beach morphodynamic state model proposed by Masselink & Short[5] for Aksa beach

The morphodynamic state of the beach is determined by plotting the values of the Ω against the RTR in the model (Fig. 6). Incorporating morphological and hydrodynamic variables, Ω and RTR can determine a sequence of distinct beach morphologies and various morphodynamic states[25].

Results and Discussion

Beach topography

The beach profile data in Figure 7 is crucial for understanding the beach morphology and its response

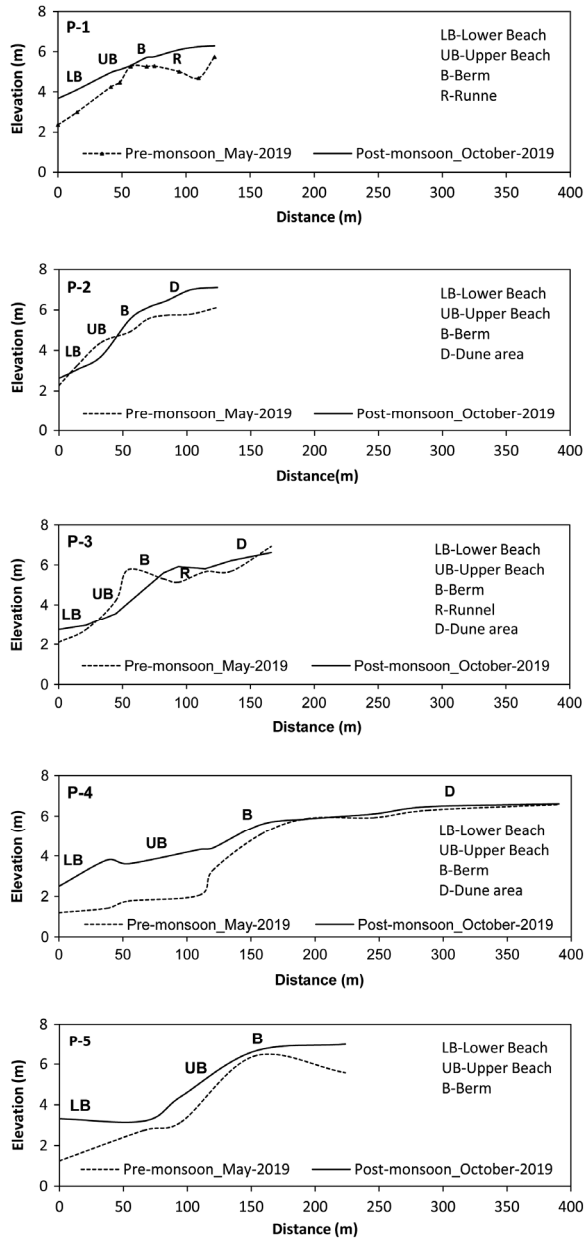

Fig. 7 — The topographic conditions of five locations (Profile 1 – 5) along Aksa beach

to different seasons. The profiles are arranged from top to bottom, showing the topography changes in pre and post-monsoon season. The figure visually represents how the elevation of beach and shape vary at these specific locations due to seasonal changes.

In the current study, the impacts of waves, tides, and currents on beach morphology were assessed on a season-wise basis. The changes in the topography of the beach over the pre and post-monsoon seasons are noted by studying the slope profiles of the beach. The major differences in the beach profiles of the two periods mentioned are mainly related to the presence or absence of the berm line and its shifting with reference to the distance from the sea. It is noted that in the post-monsoon season, the berm line shifts towards the landward side, indicating deposition and formation of berm due to low energy waves. The analysis of the data indicates that season-wise exchange of sediments takes place between the beach and the intertidal zone. In the pre-monsoon season, there is more erosion in the lower beach area than the upper beach. This results in shifting the berm line towards the seaward side. In the post-monsoon season, there is deposition on the lower beach area and the berm line shifts towards the landward side. Variations in the wave height and energy are also noted during the pre and post-monsoon seasons. In the pre-monsoon season, wave height and energy are more than that in the post-monsoon seasons.

As shown in Figure 7, the beach is found to be eroded during the pre-monsoon season and accreted during the post-monsoon season. The position of the berm shifts from the landward side to the seaward side during the pre-monsoon season. Conversely, the berm shifts towards the landward side in the post-monsoon season. The topographic data collected indicate sediment exchange occurs between the beach and nearshore area on a seasonal cycle. The most influential factors that change the morphology of the beach are waves, tides, and currents. During the post-monsoon season, lower wave energy was observed due to meteorological conditions.

Sediment analysis

According to Nelson[26], sediment sorting provides information about the relationship between sediment diameter and the average grain size of sediments. A lower sorting index indicates uniformity in sediment size, while a higher sorting index suggests heterogeneity in sediment grain size. The sorting index can determine the degree of homogeneity in a particular sediment sample, with well-sorted sediments indicating fewer subaerial processes and poorly sorted sediments indicating the role of numerous subaerial processes. Griffith[27] and Inman & Chamberlain[28] also found that better sediment sorting represents fine or coarse sediment than poor sorting sediments. The sorting index is computed using the formula $SD = (\phi\ 84 - \phi\ 16)/4 + (\phi\ 95 - \phi\ 5)/6.6$, as proposed by Folk & Ward[18].

Additionally, sediment sorting can provide information about the energy and velocity of the carrying medium from which sediments were deposited. To visualize the distribution of the sorting index, a raster surface is created using the Inverse Distance Weighting (IDW) interpolation method for the grain size values measured along the profiles. Figure 8 shows that moderately sorted 0.7 – 1.0 (ϕ)

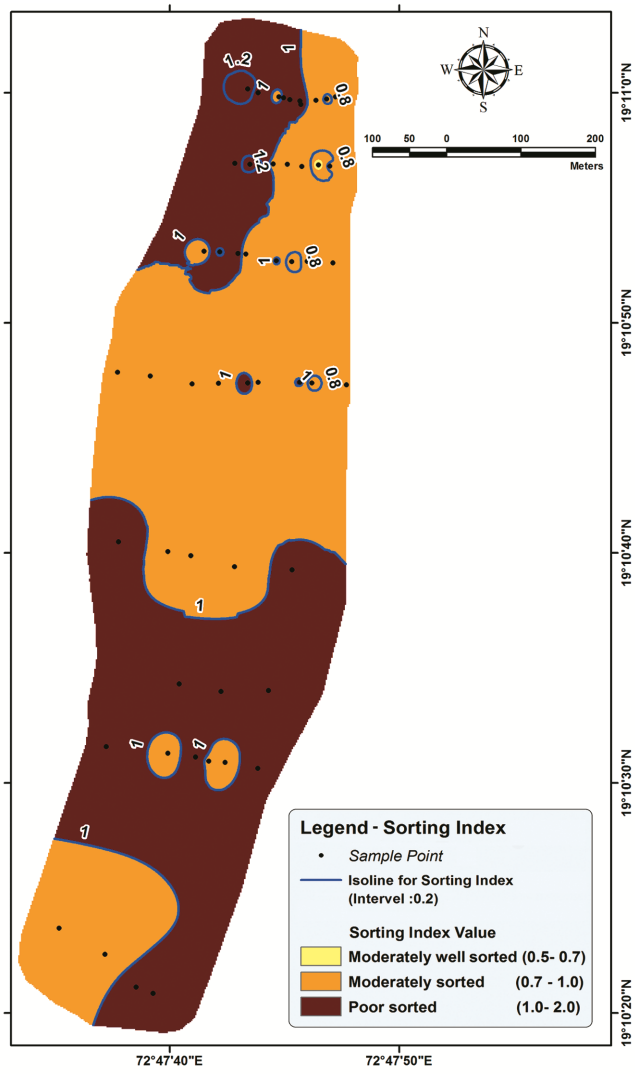

Fig. 8 — Distribution of sorting of sediment at Aksa beach

and poor sorted 1.0 – 2.0 (ϕ) are indicated by brown and dark brown colour, respectively. Moderately sorted sediments are mainly observed in the north-western part, south-central part, and southwest part of the beach, indicating particles within a relatively narrow range of sizes 1.0 – 2.0 (ϕ). Half of the beach is covered with poorly sorted sediments with the north-western lower beach part, south-central and dune zone (eastern part of the beach) and north-eastern dune zone sediments being poorly sorted.

Pradhan *et al.*[29] stated that the mean grain size is the representative diameter of coastal sediments that describes various environmental information, such as physical and geomorphological processes near the beach environment. The mean grain size is used by coastal sedimentologists to understand the origin of sediment, accretion, and erosion processes within a coastal environment. Generally, beaches exposed to high-energy waves have greater sedimentation than those exposed to lower-energy waves. Coarse sands are deposited in areas with much turbulence because the flow cannot carry enough due to the turbulence. Fine sands are carried by the flow caused by waves breaking and deposited separately in an area with weak turbulence[30]. The formula used to calculate grain size is $M = (\phi\ 16 + \phi\ 50 + \phi\ 84)/3$, as proposed by Folk & Ward[18].

Figure 9 shows the distribution of the mean grain size, which varies between 0 to 3 ϕ. Sand grain size is represented by yellow for coarse sand 0 – 1 (ϕ), brown for medium sand 1 – 2 (ϕ), and dark brown for fine sand 2 – 3 (ϕ). The coarse sand observed is only a tiny portion of the central part of the lower beach, where the grain size depends on the velocity and energy of waves. When the wave velocity is high, the grain size is medium to coarse. The major part of the beach is covered with medium median grain size sand, where waves and winds work on sediment distribution. Fine sand can be observed in the southern part of the beach. Fine sands in small circular areas result from both wave energy and micro-scale topography. It is observed that a small depression and sandbar are formed in the southern part of Aksa beach. Fine sands are deposited in low-lying circular depressions due to less wave size and energy.

Beach stage model

Identification of beach stage through classification schemes can be a helpful way to think about the different forcing mechanisms and controls that lead to the different types of beaches seen worldwide[31-33]. A large portion of the classification and modelling of the beach stage was done in Australia. Wright & Short[34] established a beach classification model that was the result of a huge body of earlier work to characterize the morphodynamic characteristics of a beach system[3,4,35,36]. Beach stage models have also been utilized as the basis for beach risk assessment due to the link between beach morphology and surf hazards to bathers[37,38] with a particular emphasis on the impact of rip currents[39,40].

One of the key parameters of the beach stage is the morphodynamic state, which was determined based on the beach slope, grain size distribution, and relative tidal range[5,31,41-43]. The beach slope is an essential factor that affects wave energy dissipation and sediment transport. The grain size distribution

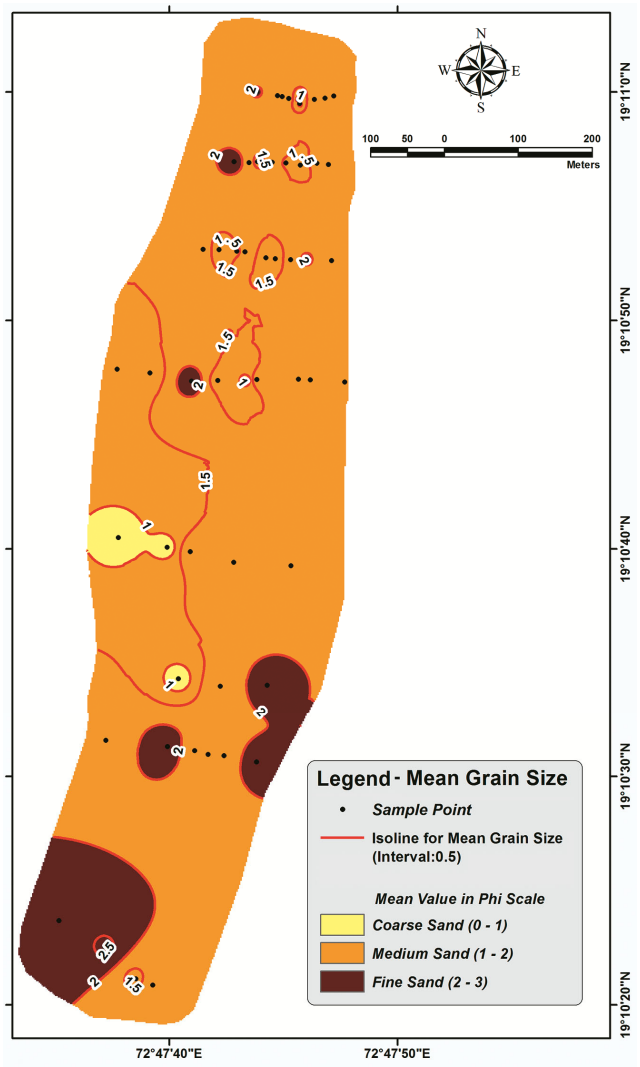

Fig. 9 — Distribution of grain size of sediment at Aksa beach

(Figs. 8 & 9) provides information about the sediment composition of the beach, which affects sediment transport and morphology. The relative tidal range (Eq. 6) also plays a crucial role in sediment transport and beach morphology. Another important parameter is the breaker wave type, which was determined based on the breaker wave height (H) and wave period (T). The average wave parameter values can be found in Table 1. The breaker wave type affects the sediment transport and morphology of the beach. Longshore bars were also considered in the beach state model, as they significantly affect wave energy dissipation and sediment transport. The relative tidal range was used to determine the presence of longshore bars. Furthermore, the fall velocity parameter was also calculated to determine the sediment dynamics of the beach. The fall velocity parameter[44] (Eq. 5) measures the settling velocity of sediment particles, which affects sediment transport and morphology.

Table 2 shows several parameters that detail the morphodynamic, hydrodynamic, and sediment dynamic properties of Aksa Beach. This table contains information that enhances our understanding of the beach's unique dynamics and serves as a useful reference for future studies and projects.

The analysis of beach profiles combined with wave data provides a clear understanding of beach topography and the physical behaviour of the coast. The morphodynamic state of the beach system can be calculated based on Wright & Short[4] morphodynamic state model. The wave parameters have been used to estimate the breaker wave type and morphodynamic state of the beach system. It includes the relation between grain size distribution and beach morphology. The results of breaker type and morphodynamic state are classified into three domains. Those are reflective, intermediate and dissipative. It is found that Aksa beach is of intermediate reflective type.

The Ω values are in the range of 2.31 throughout the year (Fig. 6). Therefore, the beach is determined as the intermediate beach state judged by Wright & Short's model. The model proves that the rip current is possible throughout the year on this beach. From the beach stage model analysis, the hydrodynamic and morphodynamic factors have been identified for drowning incidents at Aksa Beach.

Results show that the beach stage is Low Tide Bar beaches with Rip currents (LTBR). The model provides valuable information about rip currents with low tide bar occurrences throughout the year. However, the study also highlights the potential drowning hazard at Aksa beach due to its complex morphology, controlled by hydrodynamics and morphodynamics.

Table 2 — Various parameters of morphodynamic, hydrodynamic and sediment dynamics at Aksa beach

Parameters	Beach type			
	Reflective	Intermediate	Dissipative	Aksa beach (present study area)
Morphodynamic state (Wright *et al*., 1985)[42]	n < 1	1 < n < 6	n > 6	n = 0.51
Breaker wave type - Eq (4) (Resio *et al*., 2002)[24]	Surging breakers X > 2	Plunging breakers 0.4 < X < 2	Spilling breakers X < 0.4	X = 2.31 Surging breaker- reflective beach
Beach slope (Bascom,1951)[43]	Beach slope greater than 3 degree	3° – 1°	< 1°	4.75° Reflective beach
Grain size distribution (Bascom, 1951)[43]	Medium sand	Fine-medium sand	Fine sand	Medium sand-reflective beach
Breaker wave height (H) (Wright *et al*.,1985)[42]	Low wave height (H) (H < 0.5 m)	Moderate wave height (H) (0.5 < H < 1.5)	High wave height (H) (H > 1.5)	0.2 Low wave height (H) - reflective beach
Wave period (T) (Wright *et al*.,1985)[42]	More than 10 s	Between 6 and 10 s	Below 6 s	9.02 s Intermediate beach
Longshore bar (Bascom, 1951)[43]	Probably one bar or no bar present in the surf zone	At least one bar is present in the surf zone	Three or more bars present in the surf zone	At least one bar at intermediate beach
Relative tidal range (RTR) - Eq. (6) (Masselink & Short 1993)[5]	RTR < 3	(3 – 7)	> 7	4.81
Fall velocity parameter (Ω) - Eq. (5) (Komar & Gaughan's 1972)[44]	Ω < 2	Ω = 2 – 5	(Ω > 5	2.31

Conclusions

The morphodynamic state and the observable parameters such as grain size distribution, breaker wave height (Hb), wave period (T), Relative Tidal Range (RTR), fall velocity parameter (Ω), beach slope, breaker wave type and presence of longshore bar, have been analyzed for the Aksa beach. It is found that the Aksa beach is of intermediate reflective type. This identification of type is based on the existing classification of various parameters suggested by Wright & Short and Masslink & Short[4,5], with slight changes to morphodynamic indices. The existing models consider morphodynamic state, grain size distribution, H, T, RTR and Ω factors to identify beach stage. Along with these factors, the present study has included beach slope, breaker wave type and presence of longshore bar in the nearshore zone as the additional factors for identifying the beach stage.

Most parameters such as a surging breaker, medium beach slope, medium size of sand, low wave height (H), and at least one bar and LTBR (low tide bar beaches with rip current) indicate that the Aksa beach has an intermediate reflective domain, which is primarily contributed by LTBR. Therefore, the LTBR is responsible for beach drowning incidents.

In the nearshore zone of the Aksa beach, a dynamic system of longshore bars is also found. These longshore bars are formed due to excessive erosion of the beach owing to a steep slope and the resultant deposition of sediments in the nearshore zone. In turn, this modifies the interaction between the waves and the beach sediments.

Another peculiar characteristic of Aksa beach noted is the presence of sandbars is a key factor in rip current formation. These sandbars create narrow channels in the nearshore region, which become pathways for water to flow seaward. Low tide conditions affect the formation and intensity of rip currents. The sandbars thus created are not stable and keep shifting along the beach. This particular mechanism has given the beach its peculiar character of being a drowning-prone beach as the beachgoers are unaware of the channels created due to the presence of these sandbars and suddenly find themselves in the grip of the rip current. The study findings are crucial for beach safety measures and drowning prevention. Therefore, educating beachgoers and providing proper safety measures to prevent drowning accidents at Aksa beach is essential.

Acknowledgements

We thank the Office of the Brihanmumbai Municipal Corporation (BMC) lifeguards for providing information on actual beach conditions and drowning incidents. We also acknowledge the assistance of Mr Nathuram Suryabansi and Ms Anita Jaiswal for their help throughout the field survey.

Funding

The authors declare that they have not received any funding for this research.

Conflicts of Interest

The authors declare that they have no conflicts of interest regarding this research paper and have no competing or any other interests that might be perceived to influence the results and discussion reported in this paper.

Ethical Statement

The ethical considerations in the research are ensuring that the manuscript represents original work. It also ensures that the research was conducted in an ethical and responsible manner and acknowledges any potential conflicts of interest.

Author Contributions

SD wrote the main manuscript and prepared all figures and tables. DG reviewed the manuscript, provided corrections, and incorporated valuable text in the main manuscript. Both authors have contributed to the conceptualization of the study, data collection, analysis, and interpretation of results. They have also provided critical feedback and revisions throughout the writing process and have given final approval for the version to be published.

References

1 Carter R W G, *Coastal Environments*, (Academic Press Ltd, London), 1991, pp. 617. ISBN 0-12-161856-0

2 Pethick J, *An Introduction to Coastal Geomorphology*, (Edward Arnold Ltd, London), 1984, pp. 95.

3 Wright L D, Chappell J, Thorn B G, Bradshaw M P & Cowell P, Morphodynamics of a reflective and dissipative beach and inshore systems: Southeastern Australia, *Mar Geol*, 32 (1-2) (1979), 105-140.

4 Wright L D & Short A D, Morphodynamics of beaches and surf zones in Australia, In: *Handbook of Coastal Processes and Erosion*, edited by Komar P D, (CRC Press, Boca Raton), 1983, pp. 316. https://doi.org/10.1201/9781351072908

5 Masselink G & Short A D, The effect of tide range on beach morphodynamics and morphology: a conceptual beach model, *J Coast Res*, 9 (3) (1993) 785-800. https://www.jstor.org/stable/4298129

6 Gadkari D & Das S, Risk assessment of drowning incidents at Aksa Beach, Mumbai, India, *Curr Sci*, 123 (5) (2022) 687-693. https://doi.org/10.18520/cs/v123/i5/687-693

7 D'Alessandro L, Davoli L, Palmieri E L & Raffi R, Natural and anthropogenic factors of the recent evolution of the Calabria beaches, In: *Applied geomorphology: Theory and practice*, edited by Allison R J, (Wiley, New York), 2002, pp. 397–427.

8 James I D, Non-linear waves in the nearshore region: Shoaling and set-up, *Estuar Coast Mar Sci*, 2 (3) (1974) 207–234. https://doi.org/10.1016/0302-3524(74)90013-9

9 Devananth R, Anto J, Kannan S V & Manju S, Experimental Analysis of Waves Energy Spectrum Interaction on Sea wall Structures along Puducherry Coast, *J Crit Rev*, 7 (4) (2020) 1214-1218.

10 Cooper N J, Leggett D J & Lowe J P, Beach-Profile Measurement, Theory and Analysis: Practical Guidance and Applied Case Studies, *Water Environ J*, 14 (2) (2007) 79-88. https://doi.org/10.1111/j.1747-6593.2000.tb00231.x

11 Johnson D W, *Shore processes and shoreline development*, (John Wiley & Sons Ltd, New York), 1919, pp. 625.

12 Cambers G, *Coping with beach erosion*, *with Case Studies from the Caribbean*, (Coastal Management Sourcebooks, UNESCO Publishing, Paris), 1998, pp. 13–17.

13 Goudie A, *Geomorphological Techniques*, 2nd edn, (Routledge, London & NY), 1990, pp. 692.

14 Komar P D, *Beach Processes and Sedimentation*, (Prentice Hall, New Jersey), 1998, pp. 321.

15 Pentney R M & Dickson M E, Digital Grain Size Analysis of a Mixed Sand and Gravel Beach, *J Coast Res*, 28 (1) (2012) 196–201.

16 Tucker M, *Techniques in sedimentology*, (Blackwell Scientific, Oxford), 1995, pp. 394.

17 Blott S J & Pye K, GRADISTAT: A grain size distribution and statistics package for the analysis of unconsolidated sediments, *Earth Surf Proc Land*, 26 (11) (2001) 1237–1248. https://doi.org/10.1002/esp.261

18 Folk R L & Ward W C, Brazos River bar Texas, a study in the significance of grain size parameters, *J Sediment Res*, 27 (1) (1957) 3–26. https://doi.org/10.1306/74D70646-2B21-11D7-8648000102C1865D

19 Hanamgond P T & Chavadi V C, Small-scale temporal variations in morphology and grain size characteristics of the sediments of Binge Beach, India, *J Coast Res*, 8 (1) (1992) 201-209.

20 Umar H, Yuwono N, Triatmadja R & Nizam, Measurement of Long Shore Current after Permeable Groin by Floating Object, *Proc 7th Int Conf Asian Pacific Coasts*, *APAC*, (Bali, Indonesia), 2013, pp. 415.

21 Silva A, Taborda R, Rodrigues A, Duarte J & Cascalho J, Longshore drift estimation using fluorescent tracers, New insights from an experiment at Comporta Beach, Portugal, *Mar Geol*, 240 (1–4) (2007) 137–150. https://doi.org/10.1016/j.margeo.2007.02.009

22 Trujillo A P & Thurman H V, *Essentials of oceanography*, 13th edn, (Pearson, US), 2019, pp. 345.

23 Dyer K R, *Coastal and Estuaries Sediment Dynamics*, (John Wiley & Sons, New York), 1986, pp. 45.

24 Resio D T, Bratos S M & Thompson E F, Meteorology and Wave Climate, Chapter II-2, In: *Coastal Engineering Manual*, (US Army Corps of Engineers, Washington D.C), 2002, pp. 72.

25 Timothy M S, *Beach morphodynamics and associated hazards in the UK*, Ph.D. thesis, University of Plymouth, England, 2009.

26 Nelson S A, *Earth & Environmental Sciences: Physical Geology*, (Tulane University press), 2017, pp. 231.

27 Griffiths J C, Size versus sorting in some Caribbean sediments, *J Geol*, 59 (1) (1951) 211-243.

28 Inman D I & Chamberlin T K, Particle size distribution in near shore sediments, In: *Finding Ancient Shoreline*, edited by Hough J L & Menard H W, (SEPM Society for Sedimentary Geology, USA), 1955, pp. 106-126. https://doi.org/10.2110/pec.55.01

29 Pradhan U K, Sahoo R K, Pradhan S, Mohanty P K & Mishra P, Textural Analysis of Coastal Sediments along East Coast of India, *J Geol Soc India*, 95 (2020) 67-74. https://doi.org/10.1007/s12594-020-1387-2

30 Jiang C, Wu Z, Chen J, Deng B & Long Y, Sorting and Sedimentology Character of Sandy Beach Under Wave Action, *Procedia Eng*, 116 (2015) 771-777. https://doi.org/10.1016/j.proeng.2015.08.363

31 Short A D & Jackson D W T, Beach Morphodynamics, In: *Treatise on Geomorphology*, edited by John F Shroder, (Academic Press, Cambridge, Massachusetts), 2013, pp. 106-129. https://doi.org/10.1016/B978-0-12-374739-6.00275-X

32 Scott T, Masselink G & Russell P, Morphodynamic characteristics and classification of beaches in England and Wales, *Mar Geol*, 286 (1–4) (2011) 1–20. https://doi.org/10.1016/j.margeo.2011.04.004

33 Loureiro C, Ferreira O & Cooper J A G, Applicability of parametric beach morphodynamic state classification on embayed beaches, *Mar Geol*, 346 (2013) 153–164. https://doi.org/10.1016/j.margeo.2013.09.005

34 Wright L D & Short A D, Morphodynamic variability of beaches and surf zones, a synthesis, *Mar Geol*, 56 (1-4) (1984) 92–118. https://doi.org/10.1016/0025-3227(84)90008-2

35 Short A D, Multiple offshore bars and standing waves, *J Geophy Res*, 80 (27) (1975) 3838–3840. https://doi.org/10.1029/JC080i027p03838

36 Short A D, Wave power and beach-stages, A global model, *Proc 16th Int Conf Coast Eng*, (Hamburg, ASCE, Reston, Virginia), 1978, pp. 1145–1162.

37 Short A D, *Beaches of the New South Wales Coast*, 2nd edn, (Sydney University Press, Sydney, Australia), 2007, pp. 367.

38 Short A D, *Beach and Shoreface Morphodynamics*, (Wiley, Chichester), 1999, pp. 379.

39 Short A D & Hogan C, Rip currents and beach hazards: their impacts on public safety and implications for coastal management, *J Coast Res*, 12 (12) (1994) 197–209.

40 Scott T M, Russell P E, Masselink G & Wooler A, Rip current variability and hazard along a macro-tidal coast, *J Coast Res*, 56 (2009) 895–899.

41 Short A D, The role of wave height, period, slope, tide range and embaymentisation in beach classifications: A review, *Rev Chil Hist Nat*, 69 (1996) 589-604.

42 Wright L D, Short A D & Green M O, Short-term changes in the morphodynamic state of beaches and surf zones, an empirical predictive model, *Mar Geol*, 62 (3-4) (1985) 339–364. https://doi.org/10.1016/0025-3227(85)90123-9

43 Bascom W N, Characteristics of natural beaches, In: *Proc of the 4th International Conference on Coastal Engineering*, (American Society of Civil Engineers Chicago, Illinois), 1954, pp. 163-180.

44 Komar P D & Gaughan M K, Airy wave theory and breaker height prediction, In: *Proc of 13th Coastal Engineering Conference*, (Vancouver, Canada), 1972, pp. 405–418. https://doi.org/10.9753/ICCE.V13.20